vanG Element Insertions within a Conserved Chromosomal Site Conferring Vancomycin Resistance to *Streptococcus agalactiae* and *Streptococcus anginosus*

Velusamy Srinivasan,[a] Benjamin J. Metcalf,[a] Kristen M. Knipe,[b] Mahamoudou Ouattara,[a] Lesley McGee,[a] Patricia L. Shewmaker,[a] Anita Glennen,[c] Megin Nichols,[d] Carol Harris,[e] Mary Brimmage,[e] Belinda Ostrowsky,[f] Connie J. Park,[f] Stephanie J. Schrag,[a] Michael A. Frace,[b] Scott A. Sammons,[b] Bernard Beall[a]

Centers for Disease Control and Prevention, Division of Bacterial Diseases, Respiratory Diseases Branch, Atlanta, Georgia, USA[a]; Division of Scientific Resources, Biotechnology Core Facility Branch, Centers for Disease Control and Prevention, Atlanta, Georgia, USA[b]; Minnesota Department of Public Health, Stillwater, Minnesota, USA[c]; New Mexico Department of Health, Santa Fe, New Mexico, USA[d]; Jacobi Medical Center, Bronx, New York, USA[e]; Montefiore Medical Center and Albert Einstein College of Medicine, New York, New York, USA[f]

V.S. and B.J.M. contributed equally to this article.

ABSTRACT **Three vancomycin-resistant streptococcal strains carrying *vanG* elements (two invasive *Streptococcus agalactiae* isolates [GBS-NY and GBS-NM, both serotype II and multilocus sequence type 22] and one *Streptococcus anginosus* [Sa]) were examined. The 45,585-bp elements found within Sa and GBS-NY were nearly identical (together designated *vanG-1*) and shared near-identity over an ~15-kb overlap with a previously described *vanG* element from *Enterococcus faecalis*. Unexpectedly, *vanG-1* shared much less homology with the 49,321-bp *vanG-2* element from GBS-NM, with widely different levels (50% to 99%) of sequence identity shared among 44 related open reading frames. Immediately adjacent to both *vanG-1* and *vanG-2* were 44,670-bp and 44,680-bp integrative conjugative element (ICE)-like sequences, designated ICE-r, that were nearly identical in the two group B streptococcal (GBS) strains. The dual *vanG* and ICE-r elements from both GBS strains were inserted at the same position, between bases 1328 and 1329, within the identical RNA methyltransferase (*rumA*) genes. A GenBank search revealed that although most GBS strains contained insertions within this specific site, only sequence type 22 (ST22) GBS strains contained highly related ICE-r derivatives. The *vanG-1* element in Sa was also inserted within this position corresponding to its *rumA* homolog adjacent to an ICE-r derivative. *vanG-1* insertions were previously reported within the same relative position in the *E. faecalis rumA* homolog. An ICE-r sequence perfectly conserved with respect to its counterpart in GBS-NY was apparent within the same site of the *rumA* homolog of a *Streptococcus dysgalactiae* subsp. *equisimilis* strain. Additionally, homologous *vanG*-like elements within the conserved *rumA* target site were evident in *Roseburia intestinalis*.**

IMPORTANCE **These three streptococcal strains represent the first known vancomycin-resistant strains of their species. The collective observations made from these strains reveal a specific hot spot for insertional elements that is conserved between streptococci and different Gram-positive species. The two GBS strains potentially represent a GBS lineage that is predisposed to insertion of *vanG* elements.**

Received 5 June 2014 **Accepted** 19 June 2014 **Published** 22 July 2014

Citation Srinivasan V, Metcalf BJ, Knipe KM, Ouattara M, McGee L, Shewmaker PL, Glennen A, Nichols M, Harris C, Brimmage M, Ostrowsky B, Park CJ, Schrag SJ, Frace MA, Sammons SA, Beall B. 2014. *vanG* element insertions within a conserved chromosomal site conferring vancomycin resistance to *Streptococcus agalactiae* and *Streptococcus anginosus*. mBio 5(4):e01386-14. doi:10.1128/mBio.01386-14.

Editor James Hughes, Emory University School of Medicine

Address correspondence to Bernard Beall, bbeall@cdc.gov.

This article is a direct contribution from a Fellow of the American Academy of Microbiology.

Documented streptococcal resistance to the glycopeptide antibiotic vancomycin has until very recently been restricted to single reports in *Streptococcus mitis*, where a genetic basis was not defined (1), and in *Streptococcus bovis*, where *vanB*-conferred resistance was described (2). In early 2013, the isolation of two independent vancomycin-resistant group B streptococcal (GBS) strains that gave positive results in a *vanG* PCR assay was described (3). Unexpectedly, comparisons of the *vanG* gene and immediately flanking open reading frames (orfs) from these two GBS strains revealed considerable divergence, even though the two strains shared the same capsular serotype and multilocus sequence type. The complete *vanG* element sequences and chromosomal insertion regions of these two GBS strains and corresponding region from a *vanG*-positive *Streptococcus anginosus* strain are the focus of this paper.

Vancomycin and other glycopeptides bind to D-alanine–D-alanine (D-Ala-D-Ala) termini of peptidoglycan precursors, which prevents transglycosylation and transpeptidation reactions of peptidoglycan synthesis. The *vanG* operon, situated on the 3′ region of functional *vanG* elements described to date (4–8), confers

vancomycin resistance in strains of *Enterococcus faecalis* through the synthesis of peptidoglycan precursors with C-terminal D-Ala–D-serine (D-Ala-D-Ser) residues that have low vancomycin affinity while concurrently directing the removal of precursors ending with D-Ala-D-Ala. The *vanG* resistance proteins include the *vanG*-encoded D-Ala-D-Ser ligase, the *vanT*-encoded serine racemase, the *vanXY*-encoded bifunctional D,D-carboxypeptidase/D,D-peptidase, and the *vanY*-encoded D,D-carboxypeptidase which in some elements may be inactive due to a frameshift mutation (5). Detailed transcriptional analysis of a *vanG* operon in *E. faecalis* and assessment of *vanG* product enzymatic activities have been previously described (5). Although *vanG*-like elements with relatively divergent sequences in comparison to *E. faecalis vanG* elements are found within *Clostridium* and *Ruminococcus* (9, 10), functional *vanG* elements shown to confer vancomycin resistance have been characterized only from a small number of *E. faecalis* strains recovered in Australia and Canada (4–7). Here we provide a preliminary description of the first known isolates of *Streptococcus agalactiae* and *Streptococcus anginosus* that express vancomycin resistance. These three strains are also the first known members of the genus *Streptococcus* that carry elements of the *vanG* type.

RESULTS

Transferability of *vanG-1* and *vanG-2*. Many attempts were made to detect transfers of these elements from the three streptococcal strains; however, all were unsuccessful. These included interspecies transfers (GBS-NY and GBS-NM donors to *E. faecalis* recipients; *S. anginosus* urine isolate [Sa] donor to *E. faecalis* and GBS recipients). Intraspecies transfer events employing GBS-NM and a diverse set of erythromycin-resistant GBS strains were also attempted. Since strains GBS-NY and GBS-NM are both serotype II and genotype sequence type 22 (ST22), it appeared possible that strain GBS6 (also serotype II and ST22) would be an ideal recipient strain for *vanG* element transfer events; however, no vancomycin-resistant recipients were detected.

Insertional inactivation of *vanG*. Inactivation of the *vanG* gene in GBS-NY was facilitated by transforming the strain to chloramphenicol resistance with plasmid pVE6007-G′ via a single-crossover event. This conferred a vancomycin-susceptible (MIC, <1.0 μg/ml) phenotype. The vancomycin-sensitive phenotype was reversible at a low frequency, and vancomycin-resistant colonies were detected following overnight growth at 37°C in Todd-Hewitt broth (THB) without drug and plating on TH agar containing 2 μg/ml vancomycin. Insertional inactivation and homologous excision events were verified through PCR employing appropriate primers annealing to *vanG* and pV6007-G′ sequences.

Resistance phenotypes. GBS-NY, GBS-NM, and *S. anginosus* strain Sa exhibited a vancomycin MIC of 4.0 μg/ml and were tetracycline resistant. Despite the observed relatedness between GBS-NY and GBS-NM (both multilocus sequence type 22, serotype II), only GBS-NY was resistant to erythromycin and clindamycin. As previously described for *vanG*-positive *E. faecalis* (5), all three streptococcal strains displayed inducible vancomycin resistance in that growth in the presence of 2 μg/ml vancomycin was accelerated by preincubation in the presence of a subinhibitory (0.4 μg/ml) concentration of the antibiotic (Fig. 1). As previously described in a report of an *E. faecalis* study (4), these *vanG*-positive strains were susceptible to the glycopeptide teicoplanin (data not shown). Growth in the presence of 2 μg/ml vancomycin was detected in GBS-NM within 2 h; however, preincubation with 0.4 μg/ml shortened this time period to 1.5 h. In contrast, detectable growth of both GBS-NY and Sa was observed only under noninducing conditions after 8 and 10 h, respectively, and these time periods were reduced under inducing conditions to 6 and 8 h, respectively. *E* test results revealed that strains GBS-NY and Sa had a vancomycin MIC of 3.5 μg/ml, while GBS-NM had a slightly higher MIC of 4.0 μg/ml. The broth dilution vancomycin MIC for all 3 strains was 4.0 μg/ml.

Growth rate and β-lactam susceptibility comparisons of GBS-NY with a *vanG*-inactivated derivative. To determine if there is an easily detectable growth disadvantage conferred by the *vanG-1* element, growth rates of GBS-NY were compared to those of its derivative, the pVE6007-G′ insertion strain, and to the plasmid-excised revertant of the latter strain in nonselective Todd-Hewitt broth supplemented with 1% yeast extract (THYB). We also retested the antimicrobial profiles for these three strains, primarily to determine if *vanG* conferred hypersensitivity to β-lactam antibiotics as previously described for vancomycin-resistant *Staphylococcus aureus* laboratory mutants (11). Growth and MIC comparison experiments were performed in parallel in the presence and absence of a subinhibitory vancomycin concentration (0.04 μg/ml). In brief, no significant differences in growth rates or in MICs of any antibiotics were observed. These included susceptibilities to the β-lactam antibiotics ampicillin (range of 0.12 to 0.25 μg/ml), cefazolin (0.25 μg/ml), cefoxitin (range of 4 to 8 μg/ml), penicillin (range of 0.06 to 0.12 μg/ml), and cefotaxime (range of 0.06 to 0.12 μg/ml); those values, while not indicative of basal sensitivities, are not unusual in our population-based surveillance (data not shown). The lowest MICs possible that were detectable in these assays were ≤0.008 μg/ml (ampicillin, penicillin), ≤0.004 μg/ml (cefotaxime), ≤0.016 μg/ml (cefoxitin), and ≤0.015 μg/ml (cefazolin).

Features of *vanG* operons from *vanG-1* and *vanG-2*. The 7,927-bp 8-gene *vanG* operon (Fig. 2) from GBS-NY and Sa (orf29 to orf36) shared complete sequence identity (see Table S1 in the supplemental material) with the previously described operon from *Enterococcus faecalis* strain G1-0247 (7), consisting of a previously mapped constitutively transcribed sigma^{70}-type promoter (5) 29 bp upstream of a 3-gene (*vanU*, *vanR*, and *vanS*) transcriptional regulatory region and a 5-gene (*vanY*, *vanW*, *vanG*, *vanXY*, and *vanT*) resistance region previously found to be under the control of a vancomycin-inducible promoter (5). The sequence also shared near-identity with the corresponding sequence from *E. faecalis* BM4518; however, BM4518 contained a T frameshift insertion within *vanY* (5).

GBS-NY and GBS-NM contained *vanG* elements (designated *vanG-1* and *vanG-2*, respectively) that differed considerably in size (45,585 bp versus 49,319 bp) and in sequence (Fig. 2; see also Table S1 in the supplemental material). The 7,667-bp *vanG* operon within *vanG-2* differed substantially from the corresponding 7,927-bp *vanG-1* sequence from GBS-NY, especially within the regulatory gene region (see Table S1 [compare orf29 to orf31 of *vanG-1* with orf29 to orf31 of *vanG-2*]). From *vanG-2*, the deduced first 10 VanUR amino acids shared identity to the predicted *vanG-1* VanU N terminus, followed by 10 unrelated amino acids fused to a 236-residue sequence with 61% identity to the corresponding 236 residues of the GBS-NY/Sa VanR protein (66.8% DNA sequence identity shown in Table S1). The putative

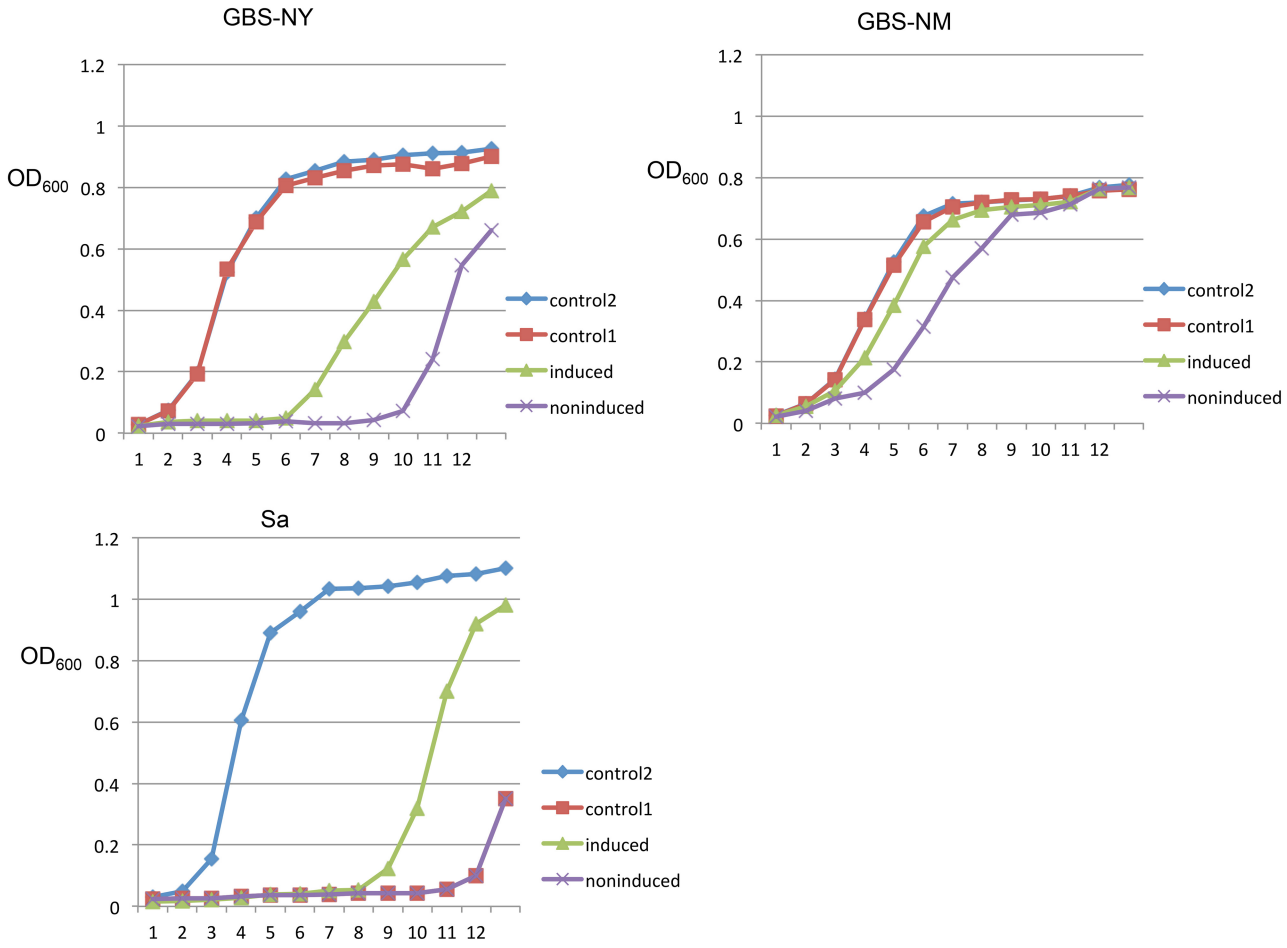

FIG 1 Growth curves for three streptococcal strains carrying *vanG* elements. control1, preincubation for 1 h at 37°C in Todd-Hewitt broth containing 0.2% yeast extract (THBY) and a subinhibitory concentration (0.4 μg/ml) of vancomycin prior to diluting the solution back to an A_{600} of 0.02 in the same medium; control2, preincubation in THBY for 1 h prior to diluting the solution back in same medium; induced, preincubation for 1 h at 37°C in THBY prior to diluting the solution back to an A_{600} of 0.02 in THBY containing 2 μg/ml vancomycin; noninduced, preincubation for 1 h at 37°C in Todd-Hewitt broth containing 0.2% yeast extract (THBY) and a subinhibitory concentration (0.4 μg/ml) of vancomycin prior to diluting the solution back to an A_{600} of 0.02 in THBY containing 2 μg/ml vancomycin. *x* axis values indicate elapsed time in hours.

sigma^{70}-directed promoter sequence, 34 bp upstream of *vanUR*, shared 72.4% identity with the corresponding *vanG-1* promoter sequence, with a −10 region perfectly matching the consensus prokaryotic sigma^{70}-directed promoter (Fig. 2). Immediately upstream of the GBS-NM *vanY* gene was a sequence with homology (20 of 29 matching positions) to the putative vancomycin-inducible promoter in GBS-NY and Sa. These results indicate that it is likely that *vanG* operon products from these streptococcal strains are transcriptionally regulated in the same manner as previously described in *E. faecalis* (5), where a constitutive promoter lies upstream of the *vanU*, *vanR*, and *vanS* (*vanUR* and *vanS* in GBS-NM) transcriptional regulatory genes and a vancomycin-inducible promoter upstream of *vanY* further directs transcription of the resistance enzyme genes.

The 5 resistance genes from GBS-NM shared progressively increased homology with their GBS-NY/Sa counterparts toward the 3′ end, with the two downstream genes *vanXY* and *vanT* sharing 95.7% and 99.5% sequence identity, respectively. The *vanG* genes shared 91% identity, with both containing codons at positions (D243, F252, and R324) postulated to be molecular determinants of terminal D-serine selectivity (12).

Additional features of *vanG-1* and *vanG-2*. Different sections of *vanG-1* and *vanG-2* displayed markedly differing GC/AT ratios, suggesting at least two different origins for components of these elements. Bases 1 to 33,205 of *vanG-1* revealed a G+C content of 47.8%, while the *vanG* operon itself (bases 33,382 to 41,308 in Fig. 2) revealed a markedly lower G+C content of 37.2%. Similarly, bases 41,308 to 45,585 had a G+C composition of 39.9%. A similar scenario was observed for *vanG-2*. While the *vanG* operon (bases 37,378 to 45,044) had a G+C content of 35.4% and bases 45,044 to 49,321 revealed a G+C content of 40.2%, the left section (bases 1 to 37,338) had a G+C content of 45.2%.

A detailed analysis of the orfs within *vanG-1* and *vanG-2* is beyond the scope of this report; however, we do highlight certain features here. The complete 45,585-bp sequences from GBS-NY and Sa differed in only 2 positions, specifically, a missense substitution within orf8 (position 7913) with no predicted function and a synonymous substitution within orf38 (position 41,951 [Fig. 2]). Although all three strains were tetracycline resistant and GBS-NY was resistant to erythromycin and clindamycin, neither *vanG* element contained genes encoding resistance to antibiotics other than vancomycin.

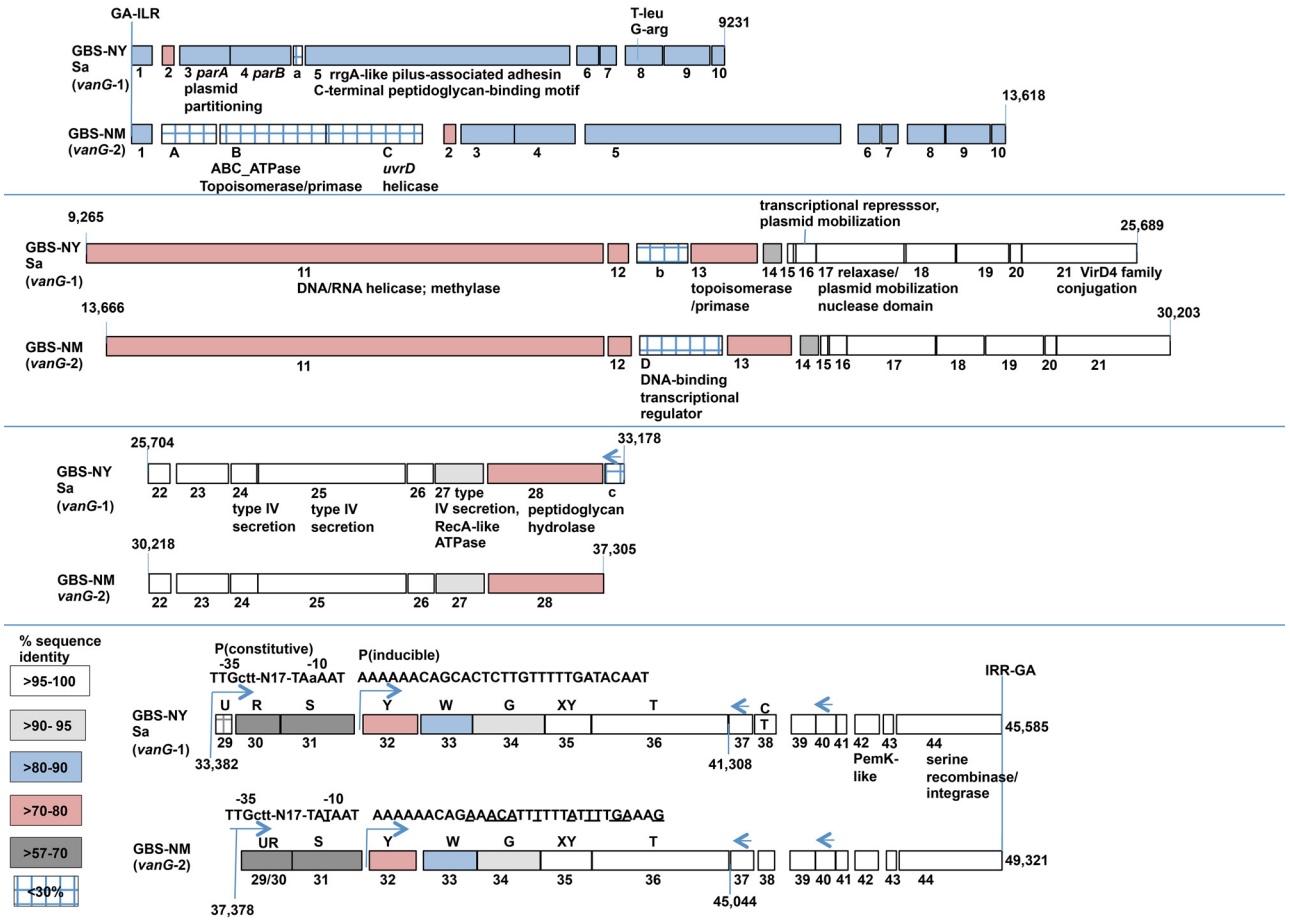

FIG 2 Diagrammatic comparison of *vanG-1* (45,585-bp) and *vanG-2* (49,321-bp) elements. The 2 differences between the two *vanG-1* elements in GBS-NY and Sa are depicted in orf8 and orf38 (the orf38 difference is translationally silent). The two elements are aligned along their entire lengths, which are shown in 4 sections, with all genes drawn to scale. The color-coded rectangles and legend indicate approximate percentages of nucleotide sequence identity between open reading frames sharing the same numbers from *vanG-1* and *vanG-2* (orf1 to orf44). Precise identity values are shown in Table S1 in the supplemental material. The base coordinates are provided at the beginning and end of each of the 4 sections. The 3 orfs within *vanG-1* that lack homologous counterparts within *vanG-2* are designated a to c. The 4 orfs within *vanG-2* that lack homologous counterparts within *vanG-1* are designated A to D. Deduced functional homologies, when observed, are indicated above specific *vanG-1* orfs (this also applies to the corresponding *vanG-2* orfs). These observations are also included in Table S1. The respective *vanG* operons in *vanG-1* and *vanG-2* are indicated as bases 33,382 to 41,308 and bases 37,378 to 45,044, respectively, each starting at the first base of the putative constitutive promoter and ending at the *vanT* stop codons. The N-terminal 10 residues deduced from orf29 and orf30 (*vanUR*) from *vanG-2* are identical to *vanU* of *vanG-1*; however, the major portion of orf29 and orf30 shares homology with *vanG-1* orf30 (*vanR*). Arrows pointing left to right in front of *vanG* operons indicate two putative promoters corresponding to previously mapped promoters in the *vanG* operon of *E. faecalis* strains WCH9 and BM4518 (5). Differences from the consensus bacterial sigma^{70} promoter are indicated in lowercase characters. The single −10 region difference in the constitutive sigma^{70} class promoter in *vanG-2* is underlined. In the same fashion, the putative vancomycin-inducible promoter sequences (5) are indicated upstream of resistance genes *vanY*, *vanW*, *vanG*, *vanXY*, and *vanT*. Arrows pointing right to left indicate orfs in the orientation opposite that of the other orfs in the diagram.

There were 47 orfs in *vanG-1*, ranging from 183 bp to 8,076 bp in length (Fig. 2; see also Table S1 in the supplemental material). Forty-four of the 47 orfs, including the *vanG* operon genes and all orfs that were >360 bp in length, were in the same orientation. Matches with >90% sequence identity to any of these orfs were not found within complete or incomplete *S. agalactiae* or *S. anginosus* genomes in NCBI databases. Forty-four of the 47 orfs, sequentially numbered orf1 to orf44 (Fig. 2), shared various degrees of homology (57% to 100% sequence identity) with corresponding orfs within the 49,321-bp *vanG-2* element from strain GBS-NM. Several of the *vanG-1* orfs shared sequence identity or high levels of homology with partially sequenced *vanG* elements from previously characterized *E. faecalis* strains (5, 7). Several of these orfs have potential roles in conjugative transposition (see Table S1).

The best overall matches to the entire *vanG-1* and *vanG-2* elements from the NCBI Nucleotide collection (nr/nt) database were from the genomes of *Roseburia intestinalis* strains XB6B4 and M50/1, respectively (see Fig. S1 and S2 in the supplemental material). Strain XB6B4 shared 34 orfs with *vanG-1*, with levels of sequence identity ranging from 60.5% to 99.4% (see Table S1 in the supplemental material). The most significant and obvious difference between *vanG-1* and this homologous element from XB6B4 was the lack of *vanG* operon regulatory and resistance genes (see Fig. S1). Of the eight *vanG* operon genes from *vanG-1*, only a relatively weakly homologous counterpart from the XB6B4 element was evident, and it was recognized to be within the *vanY*-encoded D-Ala-D-Ala carboxypeptidase superfamily (orf32 in Fig. S1 and Table S1). The *vanG-2* element and the homologous region from *R. intestinalis* strain M50/1 shared higher overall ho-

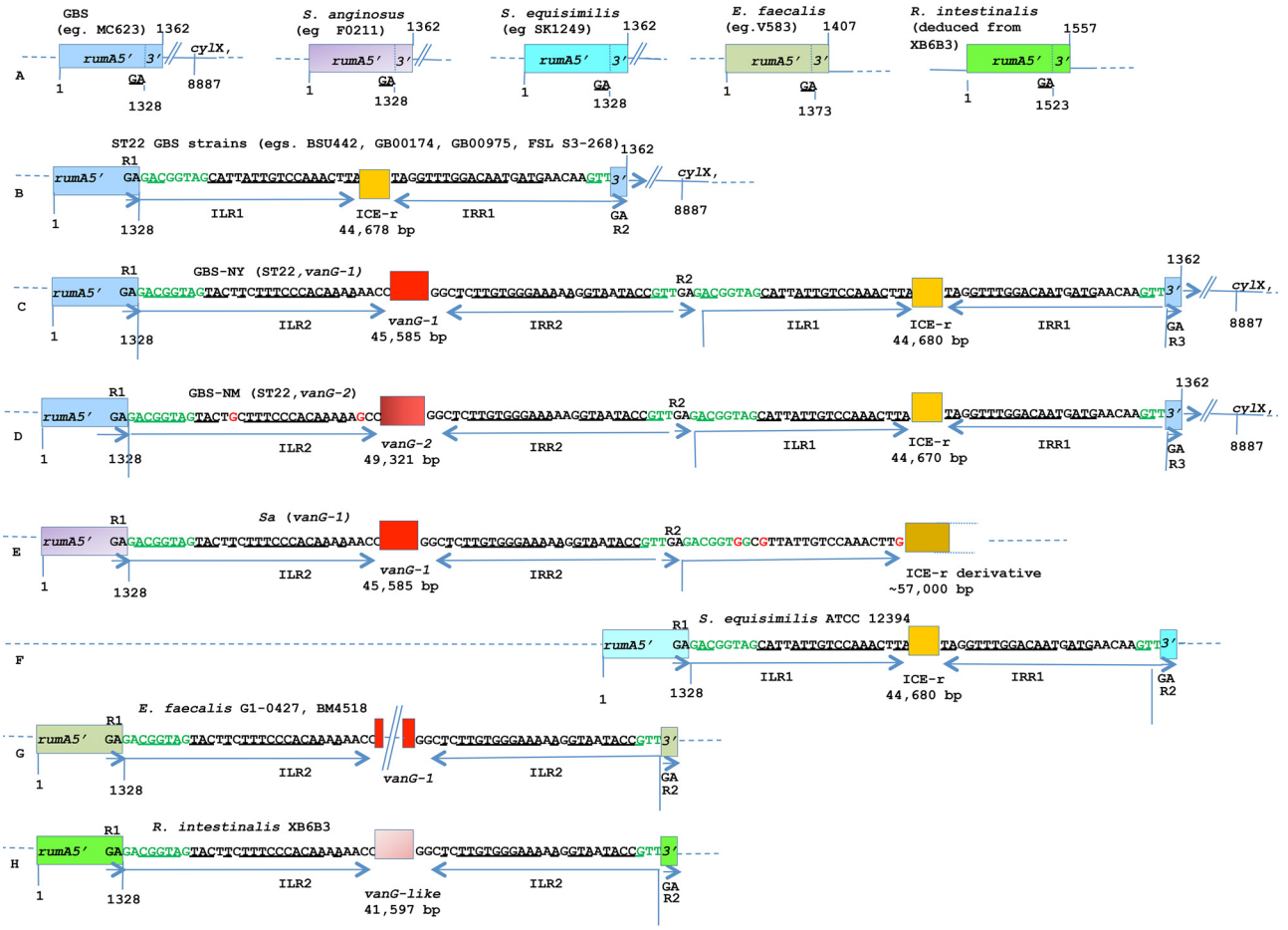

FIG 3 (A) Diagrammatic depictions of the conserved insertion target (GA) at 11th codon from the 3′ end of heterologous *rumA* genes. The differently colored *rumA* structural genes and gene segments represent the different homologs that share a deduced range of about 36% to 74% amino acid sequence identity. The conserved chromosomal location of the GBS 3′ end in relation to the hemolysin operon *cylX* gene is indicated (and is also indicated in panels B, C, and D). Genomes containing insertion elements (*vanG-vanG*-like and ICE-r/ICE-r-like) are indicated (see panels B to H). The *rumA5′* and *rumA3′* segments (see panels B to H) shared sequence identity with their overlaps in the intact *rumA* gene segments from the corresponding GenBank genome sequences indicated in panel A. (B) The ICE-r element found in ST22 GBS strains present in the NCBI wgs database. ILR1 and IRR1 indicate imperfect inverted repeats associated with ICE-r. The direct repeats of the dinucleotide target in *rumA* (GA) are also indicated (R1 and R2). The near-identical ICE-r derivative of the ST22 GBS6 study strain differs from these other isolates by a nonhomologous 12.9-kb insertion (not shown). In panels B to H, inverted repeats are underlined on both sides of 1 or 2 elements (on one side only of the ICE-r derivative shown in panel E). The 8-bp and 3-bp sequences that are shared between *vanG* and ICE-r element termini are indicated in green. (C and D) The tandem *vanG* and ICE-r insertions in strains GBS-NY and GBS-NM with the *vanG* element imperfect inverted repeats (ILR2 and IRR2) and ICE-r inverted repeats (ILR1 and IRR2). Base substitutions in the left repeat (LR) and right repeat (RR) relative to *vanG-1* are shown in red (D). (E) The *vanG-1* insertion within the *S. anginosus rumA* gene is followed by an ICE-r derivative that shares high intermittent homology with ICE-r from GBS and *S. equisimilis* ATCC 12394 (see panels B, C, D, and F). Although the *rumA* 5′ segment was identical to its counterpart in *S. anginosus* F0211 (see panel A), a corresponding ICE-r IRR1 and *rumA* 3′ segment was absent. Base changes in the unmatched ICE-r derivative inverted left repeat relative to ICE-r (panels B to D) are shown in red. (F) ICE-r element nearly perfectly conserved with GBS-NY inserted within *S. dysgalactiae* subsp. *equisimilis rumA* gene. (G) Diagram of previously published information (5, 7) describing *vanG* insertions in two different *E. faecalis* strains. The slanted vertical lines for the *E. faecalis vanG* elements indicate that the lengths are presently unknown. (H) The *vanG*-like insertion element in *R. intestinalis* XB6B3, which has high homology with *vanG-1* (see Fig. S1 in the supplemental material).

mology, with 35 orfs sharing 80% to 99.8% DNA sequence identity (see Fig. S2 and Table S1). As with the comparison of *vanG-1* with the corresponding sequence from *R. intestinalis* XB6B4, the most obvious difference between the *vanG-1* element and the corresponding sequence from *R. intestinalis* strain M50/1 was the lack of *vanG* operon counterparts, and there was no recognizable *vanY*-like orf in strain M50/1.

ICE-r and *vanG* elements in GBS are inserted within *rumA* codon 443. On the basis of comparisons to serotype II, ST22 control strain GBS6, the two heterologous *vanG* elements were inserted at the same relative positions after base 1328, within codon 443, of their identical putative RNA methyltransferase (*rumA*) genes (Fig. 3A, C, and D). Immediately downstream of both of the GBS *vanG* elements and immediately fused to the corresponding identical GBS6 *rumA* 5′ sequences was another large chromosomal element, designated ICE-r (integrative conjugative element [ICE]-like sequences) (Fig. 3B to F), with similarities to *vanG* elements that included the same apparent dinucleotide target (GA), imperfect right and left inverted repeats (ILR1 and IRR1 in Fig. 3), a homologous incomplete open reading frame at the 5′ end, and the presence of various genes potentially involved in conjugative transposition. These ICE-r genes also included a pu-

tative codon 549 serine recombinase gene situated at the right end of the element that shared 52.9% sequence identity over a 537-residue overlap of the *vanG-1* and *vanG-2* 547 codon orf44 (putative serine recombinase gene) situated at the right ends (data not shown) (note that the orf44s from the two *vanG* elements share sequence identity [see Table S1 in the supplemental material]). Although the inverted imperfect repeats of the *vanG-1* and *vanG-2* elements shared little similarity with those of the ICE-r elements (Fig. 3C and D), the first 8 bases and last 3 bases of each *vanG* element in this region were identical with those of the other Gram-positive elements shown (Fig. 3 [bases in green]). Other than a 10-base deletion within a noncoding sequence in GBS-NM, the two GBS 44,670-bp and 44,680-bp ICE-r elements shared complete sequence identity. In all three GBS strains, the ICE-r element was followed by the identical 11 *rumA* 3′ codon segment situated 7,525 bp upstream of the *cylX* gene.

The *S. anginosus vanG-1* and ICE-r-like element is inserted within codon 443 of its *rumA* homolog. We also found that the *vanG-1* element within *S. anginosus* strain Sa was inserted within a *rumA* gene completely identical over its 5′ 1,328-bp sequence with the corresponding sequence from *S. anginosus* (e.g., strain F0211) in the NCBI database (Fig. 3A and E). Immediately following the *vanG-1* direct right repeat (GA), an ICE-r derivative was evident with approximately 80% sequence identity to the GBS ICE-r; however, this homology was intermittent along approximately 57 kb of the Sa ICE-r derivative. An inverted right repeat region (IRR1) similar to that found in GBS-NY and GBS-NM was not evident in strain Sa. The full-length *S. anginosus* F0211 *rumA* gene was the typical 1,362 bases found in other streptococcal species; however, we were unable to deduce a corresponding *rumA* 3′ 11-codon sequence from strain Sa (Fig. 3A and E).

Previously reported *vanG* insertions within the *E. faecalis rumA* gene. The same relative insertion sites of *vanG* elements within a more heterologous *rumA* gene were apparent for *E. faecalis* strains G10247 and BM4518, with the separated 5′ and 3′ segments exactly matching those of the uninterrupted wild-type *E. faecalis rumA* gene (5, 7; Fig. 3A and G). These two partially sequenced *vanG* elements (GenBank accession numbers DQ212987 and DQ212986 and accession numbers AY271781 and AY271782) from *E. faecalis* shared near-identity in their overlaps with *vanG-1* from GBS-NY and Sa.

***vanG*-like and ICE-r/ICE-r insertions within the conserved *rumA* location from additional Gram-positive species.** *vanG*-like elements were observed within *R. intestinalis* genomes (see Fig. S1 and S2 in the supplemental material), and an ICE-r element nearly identical to that found within ST22 GBS was observed in *S. dysgalactiae* subsp. *equisimilis*. In all 5 species examples shown, these elements are inserted after the same dinucleotide target within the 3′ proximal 11th codon (GAG) (Fig. 3).

It was interesting that, other than the *S. agalactiae* ST22 strains, the only nearly perfectly conserved ICE-r (44,672-bp to 44,680-bp identity with GBS-NY ICE-r) was found inserted within codon 443 of the *rumA* gene in *S. equisimilis* strain ATCC 12394 (Fig. 3F). Large regions of identity to ICE-r (84% to 91% coverage, with 96% to 99% sequence identity) were also seen within *rumA* codon 443 of *S. equisimilis* strains RE378 and AC-2713, within total insertion sizes of about 60.5 kb and 98.4 kb, respectively (data not shown). A highly conserved element also observed in *Streptococcus pyogenes* is the ICESp2905 element (89% identity, 60% coverage [GenBank accession number FR691055]) inserted within its chromosomal *rumA* 3′ site (13). Within *Streptococcus equi* subsp. *equi* strain 4047, a homologous ICE-r-like derivative was also observed to be inserted within codon 443 of its *rumA* gene (GenBank accession number FM204883), with approximately 90% identity with ICE-r over a 50% overlap.

Frequent insertions within GBS *rumA* and conservation of ICE-r within ST22. The two sections of the interrupted *rumA* gene of GBS-NY, GBS-NM, and GBS6 (5′ bases 1 to 1328 and 3′ bases 1329 to 1362) exactly matched full-length 1,362-bp GBS *rumA* genes from 31 strains in the wgs (whole-genome shotgun contig) NCBI database (e.g., strain MC623). In the majority (>230) of GBS genomes, there were insertions present within this exact site. All 10 GBS whole-genome sequences within the nt/nr NCBI database contained insertions within this *rumA* site (after base 1328 within codon 443). In the majority of all GBS strains, and in all 31 genomes in the NCBI database with an intact *rumA*, the 3′ 11-codon segment of *rumA* was situated approximately 7,525 bp upstream of the *cyl* operon (data not shown) found in all hemolytic GBS strains (14, 15) (depicted in Fig. 3A to D).

Of the total of 279 *S. agalactiae* whole-genome sequences within the NCBI databases, only 12 ST22 isolates and one single-locus variant (SLV) of ST22 contained large sections of sequence identity to the GBS-NY/GBS-NM ICE-r insertions (Fig. 4), and in each isolate these sections were contained between bases 1328 and 1329 of the *rumA* gene (data not shown). Nine of the ST22 isolates contained a single ICE-r with 99% to 100% sequence identity to the ICE-r in GBS-NY, while 3 ST22 isolates (including GBS6) contained larger ICE-r derivatives containing 2 to 3 segments that together encompassed the GBS-NY ICE-r with complete sequence identity. The complete GBS6 57,583-bp ICE-r, also inserted between bases 1328 and 1329 of its *rumA* gene, contained an internal nonhomologous 12,900-bp segment (bases 23233 to 36132) that shared extensive homology (~95% identity over 5,700 bp) with mobilization genes from an *Anaerococcus prevoti* plasmid (GenBank accession number CP001709). In one ST22 strain, there were 3 interrupted sequences of near-identity to the GBS-NY ICE-r encompassed within an approximately 80-kb fragment found within the *rumA* target site. One SLV (MC633 in Fig. 4) contained an ICE-r derivative within *rumA* with 7 sections that together exactly encompassed perfect matches to 87% of the GBS-NY ICE-r (data not shown). In all three of the ST22 GBS study strains, and in all 10 ST22 genomes present in the NCBI wgs database, the GA at the start of ICE-r was followed by a left inverted repeat sequence that had a corresponding imperfect right inverted repeat at the ICE-r right end and a matching "far right" GA repeat (Fig. 3B, C, and D). Lower levels of identity (83% to 94% identity) were evident in additional strains, primarily in SLVs of ST22 (data not shown).

Observations relative to ICE-r divergence within the conserved *rumA* target site in GBS are consistent with the phylogenetic clustering of ST22 core genome sequences (Fig. 4) and with the general congruence of the core phylogeny with multilocus sequence typing (MLST). The data are consistent with the notion that ICE-r was initially introduced into ST22 GBS and subsequently diverged. It is also interesting that the two GBS-NY and GBS-NM *vanG*-positive strains were resolved together from the remaining ST22 strains in Fig. 4A, even though they contain clearly divergent *vanG* elements.

Shared features of *vanG* and ICE-r elements. It was beyond the scope of this work to investigate the nature of the *vanG* and

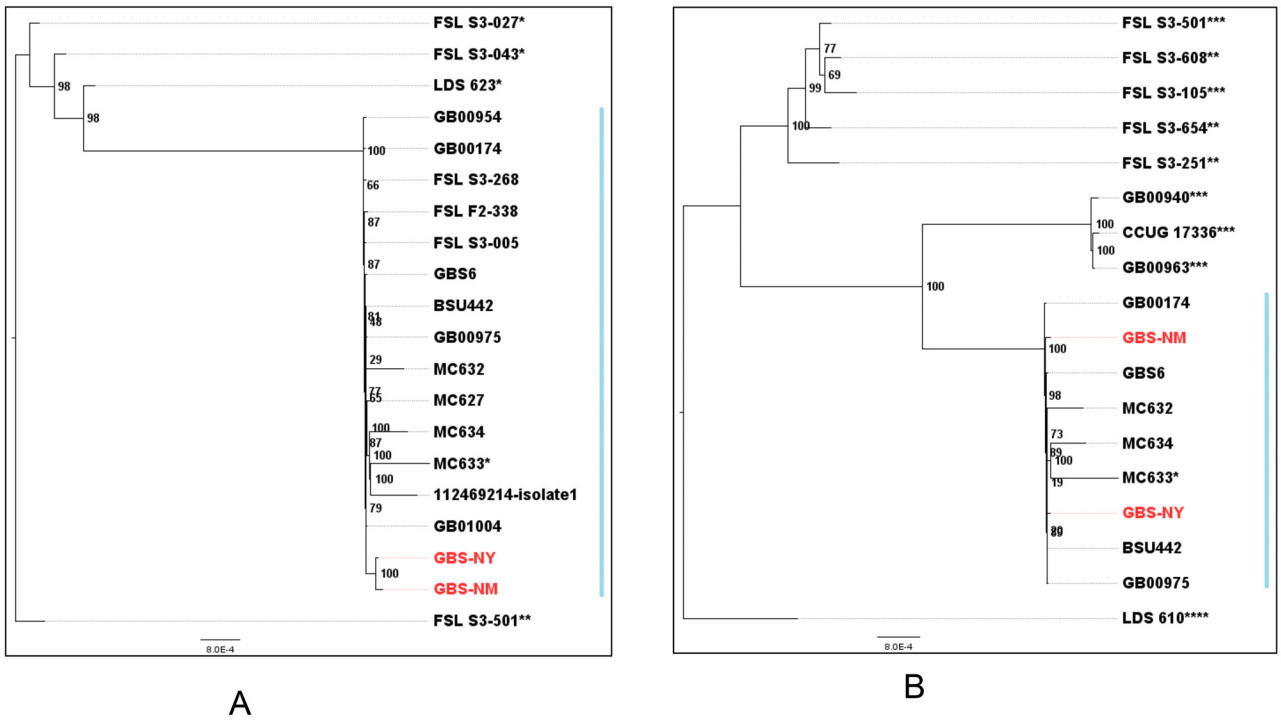

FIG 4 Comparison of core genomes of *S. agalactiae* as described in Materials and Methods, including 943 and 942 concatenated genes in panels A and B, respectively. (A) Strains aligning with the vertical blue arrows are all multilocus sequence type 22, except for one single-locus variant (SLV). MC633 and the three additional SLVs are indicated (*). FSL S3-601 is a double-locus variant (**). (B) Data were determined as described for panel A except that the comparisons of the ST22 core genomes and the SLV were made with more-divergent genomes and a different core genome to allow for the added double-locus (**), triple-locus (***), and quadruple-locus (****) variants.

ICE-r element gene content in depth; however, there are some obvious conserved features that are consistent with their shared target-site specificity. Both elements contain an array of genes homologous to previously identified genes involved in conjugative transposition. In particular, both elements contain a related 547-549 codon predicted serine recombinase/integrase gene that shares 52.8% identity in amino acid sequence (data not shown). Both putative recombinase genes encompass the right end of their element and lack a stop codon. The two elements also share homology at their left ends (Fig. 5). The *vanG* and *vanG*-related left ends are comprised of a predicted 115-codon segment, lacking a translational start, that is fused in frame to the chromosomal 5′ *rumA* gene segment. These predicted 115-amino-acid codon sequences share obvious homology with the corresponding 101 codons of ICE-r derivatives of the four streptococcal study isolates (Fig. 5A). Also depicted here is the related *R. intestinalis* strain M50/1 ICE-r derivative that lies immediately downstream of its *vanG*-like element. Although *vanG* and ICE-r share this common *rumA* gene target, and share the above-described limited homologies, their respective terminal imperfect inverted repeats are dissimilar (Fig. 3).

As a result of *vanG*-*vanG*-related and ICE-r insertions within the different Gram-positive *rumA* genes (Fig. 5), different translational fusions were generated. For strains GBS6 (and other ST22 GBS strains) and *S. equisimilis*, the *rumA* 5′ region is translationally fused to 101 codons encompassing the ICE-r left end (Fig. 3B and F and 5A). This was also true for at least one other streptococcal species in that the corresponding *rumA* 5′ region in the *S. equi* subsp. *equi* 447 strain was fused in frame in this manner, where the 101 N-terminal *rumA*–ICE-r fusion derivative residues shared 89.1% sequence identity with their counterpart ICE-r elements from ST22 GBS and *S. equisimilis* (data not shown).

Within strains containing *vanG* or *vanG*-like elements (GBS-NY, GBS-NM, *S. anginosus* strain Sa, *E. faecalis* strains G1-0427 and BM4518, *R. intestinalis* XB6B3), the *rumA* 5′ region is translationally fused to 115 codons encompassing the left end of the respective *vanG* elements (Fig. 3C, D, E, G, and H). In addition, the *rumA* 3′ 11 codon segment in all examples shown in Fig. 3, with the exception of *S. anginosus* Sa, is translationally fused to 547-549 codon putative serine recombinase genes that encompass the right ends of the *vanG*-*vanG*-like and ICE-r elements (data not shown). It was interesting, but of unknown significance, to observe the sequence similarity between the *vanG*-*vanG*-related and ICE-r portions of the two different translational fusions to the *rumA* 5′ domains (Fig. 5A), and the obvious relatedness between the 11 residue RumA termini from various Gram-positive species and the first deduced 11 residues from the various GBS insertion elements was also interesting (Fig. 5A and B). Although the *rumA* 11th 3′ proximal codon is a conserved insertion target for *vanG*-*vanG*-related and ICE-r/ICE-r-related elements in the different species shown, the reason for this is not evident on the basis of the weak interspecies *rumA* sequence homology (Fig. 6).

Numerous GBS genomes from the NCBI database displayed a diverse array of related, often short sequences translationally fused at the 3′ *rumA* target site (a partial listing of shorter deduced fusions is shown in Fig. 5C), and these were all associated with the ends of a wide variety of insertional elements. Only the coding sequence for the GBS wild-type *rumA* 3′ end (ECVALLQRSKG)

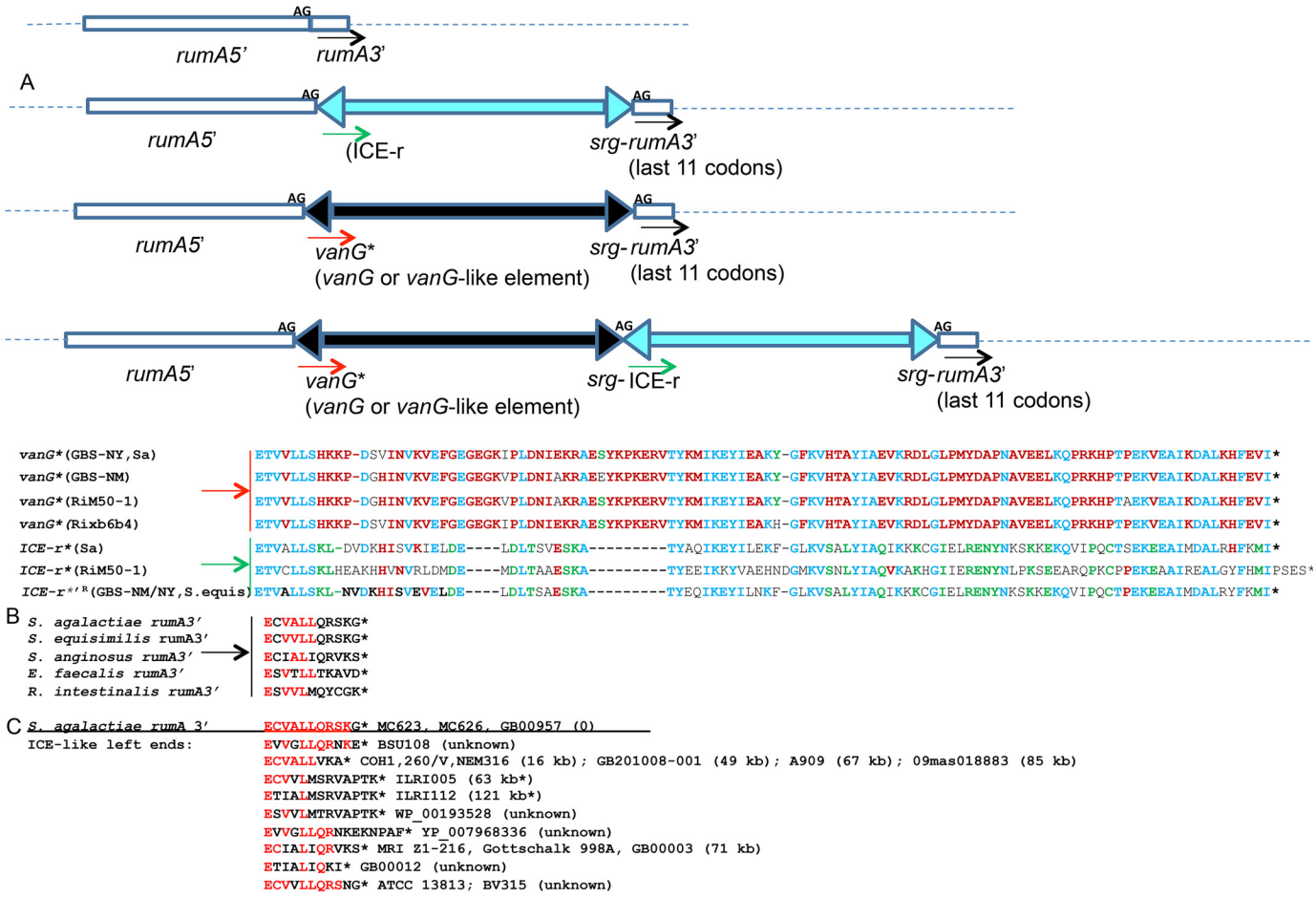

FIG 5 (A) Deduced amino acid sequence homology between the indicated left ends of *vanG-vanG*-like elements (red arrows), ICE-r elements (green arrows), and *rumA* 3′ segments (black arrows) of different translational fusions (diagrammed at the top of the panel). The residues that are completely conserved among the 7-element left ends are blue. Residues conserved in 4 to 5 left elements are red. Residues conserved among 3 elements are green. (B) The RumA C-terminal 11 residues from different species that are often translationally fused to different serine recombinase genes (srg) are directly aligned, with those conserved among the various elements shown in red. (C) Deduced related ICE-like element 5′ residues in the *S. agalactiae* NCBI database found to be fused with the wild-type chromosomal *rumA* 5′ end (below the horizontal line). Residues conserved with *S. agalactiae* wild-type *rumA* 3′ 11 codons indicated at the top (uninterrupted by an insertion element) are shown in red. Isolate identifiers or GenBank accession numbers are provided. The approximate lengths of fusion elements inserted within *rumA* are indicated in parentheses, based on the distance of the wild-type *rumA* 11 codons from *rumA* base 1328 and the *cylX* gene, consistently situated about 7,525 to 7,650 bp downstream (strains COH1, 260/V, NEM316, GB201008-001, A909, 09mas018883, and GB00003), or based on the distance of the wild-type *rumA* 11 codons from *cylX* (strains ILRI005 and ILRI112). Other strains with no lengths shown were from contigs that did not include the entire insertion element.

FIG 6 Comparisons of 4 insertion element target regions from 4 Gram-positive species with the corresponding regions in *S. agalactiae*. Percent DNA sequence identities are shown at right. Amino acid sequence identities (entire deduced RumA proteins) are shown below each alignment.

was consistently situated ~7.5 kb upstream of the *cylX* operon (either as an uninterrupted *rumA* gene or as a *rumA* gene interrupted by an insertion element). For many genomes, the deduced wild-type 5′ *rumA* 1,328-bp sequence was bisected from its 3′ 11 codons by the presence of insertional elements of various sizes (sizes of approximately 16 to 71 kb as depicted in Fig. 5C; see the fusions ending in ECVALLVKA and ECIALIQRVKS). In other genomes, the wild-type *rumA* 3′ sequence was not readily apparent; however, insertion sizes after *rumA* base 1328 were estimated on the basis of the location of the genomic *cylX* gene (strains ILRI005 and ILRI112). It is interesting that the left ends of these various elements and the apparent wild-type *rumA* gene 3′ 11 codons from various species share appreciable deduced amino acid sequence homology (Fig. 5), potentially consistent with an extensive history of insertion and excision events centering at the GBS *rumA* target.

DISCUSSION

In this report, we have described the first vancomycin-resistant strains within two different streptococcal species, *S. agalactiae* and *S. anginosus*. To our knowledge, there have been no previous validated reports of vancomycin resistance within these two species. Among more than 16,000 invasive GBS strains from Active Bacterial Core surveillance tested during 1996 to 2013, strain GBS-NM was the only isolate detected with a vancomycin MIC of 2 μg/ml or greater (unpublished data). Nonetheless, the detection of two independent vancomycin-nonsusceptible invasive GBS strains within such a limited time frame (2011 to 2012) suggests the possible emergence of vancomycin resistance within *S. agalactiae*. The implications of emergence of GBS strains with the observed level of resistance are not entirely clear. The adult patient infected with the GBS-NM strain recovered on vancomycin monotherapy (3). Vancomycin is among the agents recommended for perinatal GBS infection prevention within a very small subset of women and is rarely used (16); however, it is important that vancomycin is a common therapy for adults with mixed wound infections, which sometimes do include GBS. No growth defects were apparent in comparing the two vancomycin-resistant GBS isolates and the highly related invasive GBS6 isolate grown under laboratory conditions (data not shown) or in comparing GBS-NY and its *vanG*-inactivated insertion derivative. In addition, unlike the previously described β-lactam antibiotic hypersensitivity exhibited by laboratory-selected vancomycin-resistant *Staphylococcus aureus* mutants (11), the *vanG*-inactivated derivative of GBS-NY exhibited no increased β-lactam susceptibility. Although not conclusive, these observations are consistent with minimal or no fitness costs imposed upon streptococcal strains containing *vanG* elements.

Based upon homology to known *vanG* elements, the donors to these streptococcal strains of the *vanG* elements may be *E. faecalis* strains. From the surprising near-identity of the *vanG-1* elements (45,583 identical bases of 45,585) of the distantly related species *S. agalactiae* (strain GBS-NY) and *S. anginosus* (strain Sa), it is logical to suspect that events of transfer into these strains from a common source occurred very recently. The mechanism of *vanG* element transfer remains puzzling. The presence of imperfect inverted repeats of 28 to 30 bp on the ends of these elements is consistent with previously described conjugative elements; however, we were unable to demonstrate transfer events under laboratory conditions. In addition, conjugative transposition involves the generation of a circular intermediate. Similar to previous examination of *vanG*-positive *E. faecalis* strains, we were also unable to detect a circular form (5) (data not shown). If restricting our observations to *S. agalactiae* at the intraspecies level, the conserved location of insertion would appear potentially consistent with homologous recombination as a possible mechanism of *vanG* insertion. The *vanG-1* element, however, has obviously crossed multiple species barriers, since near-perfect copies of it exist in at least two different species, with the *vanG* operon and other segments of this element nearly perfectly conserved with previously described *E. faecalis* counterparts (5, 7). It also appears likely that *vanG* and ICE-r insertion events share the same mechanism, and in the vancomycin-resistant strains, ICE-r insertion was likely to have preceded *vanG* element insertion.

The *rumA* target specificity of *vanG*, ICE-r, and insertion elements within multiple species (5, 7), where various heterologous chromosomal *rumA* genes are interrupted through an insertion event which simultaneously reconstitutes in-frame translational fusions to *rumA* and the element-terminal serine recombinase gene, is particularly intriguing. We have not attempted here to describe the scope of what must be a very diverse array of insertion elements that are inserted within the *rumA* target. The structural basis of this cross-species conserved insertion site for the highly related *vanG-vanG*-related and ICE-r elements described here is not apparent, especially since the level of DNA sequence identity between the different *rumA* homologs is often quite low (Fig. 6). Potentially, the identical 8-bp and 3-bp termini shared between the GBS *vanG* and ICE-r elements are involved in the mysterious target site specificity of these elements.

Further analysis and comparisons of these study strains and other streptococcal genomes in the vicinity of the conserved *vanG* insertion site may lead to further insights. Analysis of the *rumA* 3′ region within *S. agalactiae* revealed a great deal of sequence variation, associated by a great diversity of introduced genetic elements that appeared to center upon this locus (Fig. 5C). The available sequence information from the various streptococcal species discussed in this paper and elsewhere (13, 17, 18), from *Roseburia intestinalis* and *E. faecalis*, and from other Gram-positive species not mentioned in this report is also consistent in the implication of this 2-base *rumA* target as a very active site for resistance-conferring insertion events among a broad range of species. The high occupancy of a diverse array of insertion elements within this specific target suggests a strategy for routine localized screening of these insertions in streptococcal and other species for the introduction of new resistances. Although not described in this report, the ICE-r like element within *S. anginosus* strain Sa contained genes predicted to confer resistance to tetracycline and aminonucleoside antibiotics.

Potentially, both *vanG* and ICE-r insertion events were mediated through serine recombinases, since both contained predicted genes on their 3′ end that share significant homology with serine recombinases, and both contain 2-bp direct repeats (GA) flanking each insertion which are representative of the target site employed by the serine recombinase family. We are unable at present to test the requirement of these or any other orfs for transfer events, since we are presently unable to facilitate *vanG* transfer events between different strains.

Analysis of the difference in G+C content between the left and right sections of both *vanG-1* and *vanG-2*, where the *vanG* operon and downstream genes display a much lower value, suggests dif-

ferent species origins for at least these sections of these elements. The role, if any, of *R. intestinalis* in the evolution of *vanG-1* and *vanG-2* elements is unclear. Despite the strong homology between *vanG-1* and *vanG-2* with corresponding *vanG*-like elements in *R. intestinalis*, it is unknown if these elements represent prior intermediates in the evolution of *vanG* elements or if they arose from functional *vanG* elements through the loss of resistance genes. The presence of these highly homologous *vanG* or *vanG*-like elements within these diverse species (*E. faecalis*, *R. intestinalis*, *S. agalactiae*, and *S. anginosus*) suggests that a very broad host range for *vanG*-conferred vancomycin resistance is conceivable.

Previous attempts to demonstrate intraspecies *vanG* element transfer either have been unsuccessful (7) or have exhibited very low transfer frequencies (5). In past successful demonstrations of intraspecies transfer in *E. faecalis*, the conserved integration site was noted for all selected recipient strains (5). The 3 different *vanG*-positive streptococcal strains clearly represent three independent acquisitions of these elements within streptococci, since two different species are represented. *E. faecalis* is likely to be the source of the *vanG-1* element in *S. agalactiae* and *S. anginosus*, since nearly identical elements have been previously documented in *E. faecalis* (5, 7) and all three species are frequently recovered from gut flora. The divergence between the two *vanG* elements found within the two serotype II, ST22 GBS strains is also indicative of independent origins; however, the identity of the donor species of the *vanG-2* in GBS-NM, which is not highly conserved throughout its length with other *vanG* elements, is open to speculation. In view of the overall high sequence similarity of *vanG-2* to a *vanG*-like element in *R. intestinalis* strain M50/1 (see Fig. S2 in the supplemental material), as well as of the near-identity shared by the *vanXY* gene, the *vanT* gene, neighboring genes, and the putative orf44-encoded serine recombinase of both streptococcal *vanG* elements, it is likely that multiple gut species have contributed to the evolution of *vanG-2*.

Our first analysis of whole-genome sequences from these three strains has not yet shed light upon the origins of these elements and the circumstances allowing for their transfer into streptococci. The coincidence of the two different elements residing within two highly related invasive GBS strains sharing the same serotype and multilocus sequence type suggests that this lineage might have specific features conducive to receiving *vanG* and related elements. It is possible that prior acquisition of the ICE-r element within the ST22 lineage made subsequent acquisition of *vanG* elements possible through providing cellular machinery necessary for the process.

MATERIALS AND METHODS

Strains. *S. anginosus* strain 2182 (Sa) was recovered from a catheterized urine specimen on 3 June 2012 from a quadriplegic in a long-term-care facility. The patient, a young woman, was involved in a motor vehicle accident in October 2011 and was treated with vancomycin for most of the hospitalization. She was later treated preoperatively with vancomycin for insertion of a ventriculoperitoneal shunt during May 2012. In early June 2012, she presented with fever and vomiting. The patient was again treated with vancomycin, and the shunt was removed. Urine culture yielded *Streptococcus anginosus* on 3 June. Subsequent urine cultures tested negative. She also had a reported history of methicillin-resistant *Staphylococcus aureus* (MRSA) (unknown dates) and may have been treated with vancomycin then as well. The identification of *S. anginosus* was confirmed using conventional biochemical identification schema, the rapid ID32 Strep identification system (bioMérieux, Inc.), and 16S rRNA gene sequencing as previously described (19). Case reports associated with the two independent invasive *S. agalactiae* isolates (designated GBS-NY and GBS-NM), recovered in two different states (New York and New Mexico) during 2011 and 2012, respectively, have been recently published (3). These two strains, GBS-NY and GBS-NM, were both serotype II, multilocus sequence type 22 (ST22), and vancomycin nonsusceptible. GBS6, an invasive vancomycin-susceptible, serotype II, ST22 control GBS strain, was recovered in New York during 2009 through CDC's Active Bacterial Core surveillance.

Resistance phenotypes. Susceptibility testing of GBS-NY and GBS-NM using the broth microdilution method (20) has been previously described (3), employing an in-house panel that was provided by Trek Diagnostic Systems. Here we additionally performed *E* tests (bioMérieux, Inc.). Strain Sa was tested using the same methods. All 3 strains were tested for inducible vancomycin resistance by preincubation for 1 h at 37°C in Todd-Hewitt broth containing 0.2% yeast extract and containing a subinhibitory concentration (0.4 μg/ml) of vancomycin prior to dilution back to an optical density (OD; absorbance at 600 nm [A_{600}]) of 0.02 in the same medium containing 2 μg/ml vancomycin. The A_{600} was measured every 60 min over a 13-h period.

***Streptococcus agalactiae* multilocus sequence typing.** The 7-locus multilocus sequence type of GBS-NY, GBS-NM, and GBS6 was determined as described at http://pubmlst.org/sagalactiae/.

As previously described (3), initial detection of the *vanG* element in all 3 strains employed PCR with the previously described EG1 and EG2 primers (6).

Genome sequencing. Initially, by employing Sanger sequencing and amplification/sequencing primers derived from data corresponding to GenBank accession numbers DQ212987 and DQ212986, ~15-kb sequences comprised of the *vanG* right and left regions from Sa and GBS-NY were obtained (data not shown). Due to the relative divergence of the GBS-NM *vanG-2* element, the original sequencing strategy employed a previously described unidirectional PCR/sequencing strategy (21), resulting in the sequence of an equivalent ~15-kb region. The left and right chromosomal junctions of the three *vanG* elements were amplified and sequenced using unidirectional PCR primers also derived from data corresponding to GenBank accession numbers DQ212987 and DQ212986, describing the left and right ends of the *vanG* element, respectively (7). Subsequently, the whole genomes from these 3 vancomycin-resistant strains, as well as GBS control strain GBS6, were sequenced employing the complementary PacBio and Illumina platforms. Sequence comparisons of the *vanG* elements, ICE-r regions, and component open reading frames employed the NCBI Blast server (http://blast.ncbi.nlm.nih.gov/Blast.cgi) and Protein Homology/analogY Recognition Engine V. 2.0 (http://www.sbg.bio.ic.ac.uk/~phyre2/html/page.cgi?id=index).

Phylogenetic comparisons of GBS core genomes. Two different data sets were used to compare the core sequences of the *vanG*-positive GBS strains to those of other related *S. agalactiae*. The first data set was comprised of the three study GBS strains (GBS-NY, GBS-NM, and GBS6), 12 additional ST22 genomes, 4 single-locus variants (SLVs) of ST22, and a single two-locus variant. The second data set contained the 3 GBS study strains, 6 additional ST22 SLVs, eight 2- to 3-locus variants of ST22, and a single 4-locus variant. The full-length genomes of *S. agalactiae* ST22 and ST22-related variants were retrieved from the NCBI ftp site (ftp://ftp.ncbi.nih.gov/genomes/). For any assemblies that did not contain the GenBank "locus_tag" gene identifiers, *de novo* predictions were performed by Prodigal V 2.60 (22) with the -c option. PanOCT ver 1.9 (23) was used to find orthologous genes that shared at least 40% sequence identity (determined by an all-against-all blastp search) (24) and 70% coverage across the genomes in each group. PanOCT found 942 orthologous genes in first data set and 943 orthologs in the second. Amino acid sequences from each core genome cluster were concatenated and aligned using FSA version v 1.15.8 (25) [with the -anchored and -nolearn options]. Finally, after removing poorly aligned regions with trimAl 1.2rev59 (26) (with the -automated1 option), maximum-likelihood analysis was carried out by the use of

RaxML v 7.3.0 (27) and a PROTGAMMAJTTF protein substitution model. Node support was assessed using 500 bootstrap replicates.

Electrocompetent GBS-NY. GBS-NY was grown overnight in 10 ml Todd-Hewitt broth supplemented with 1% yeast extract and 20-mM glycine (THYB-glycine). The overnight culture was then diluted 1/20 in 100 ml THYB-glycine (5-ml overnight culture transferred to 100 ml THYB-glycine) and incubated at 37°C without shaking under 5% CO_2. The optical density at 600 nm (OD_{600}) was monitored, and at OD_{600} = 0.3, the cells were harvested by centrifugation at 5,000 × *g* for 20 min at 10°C. The cell pellet was washed with 225 ml prechilled double-distilled water (ddH_2O), followed by a wash with 225 ml prechilled 15% glycerol and 2 successive washes with 35 ml prechilled 15% glycerol. Cells were spun at 6,000 × *g* for 15 min at 4°C between washes. The pellet was resuspended in 1.5 ml of 15% cold glycerol and divided into Eppendorf tubes as 70-μl aliquots. The aliquots were immediately frozen in dry ice and stored at −80°C.

Insertional inactivation of *vanG-1*. Campbell-type insertional inactivation of the *vanG* gene was carried out by transforming GBS-NY electrocompetent cells with a derivative plasmid of the temperature-sensitive pVE6007 plasmid (28), designated pVE6007-G′, that contained a 630-bp *vanG* internal structural gene fragment downstream of the chloramphenicol resistance gene. The pVE6007-derived plasmid was constructed by using an In-Fusion HD cloning kit (Clontech PT5162-1). A linear pVE6007 was derived using PCR with the following pair of primers: pVE6007-Fwd (GATCCACTAGTTCTAGAGCGGCC) and pVE6007Rev (ACCGTCGACCTCGAGGGG). The 630-bp *vanG* gene internal segment was amplified from GBS-NY with the following pair of primers: VG-pVE6007-Fwd (CCCCTCGAGGTCGACTTGTCGTTTCCCAAAATC GTT) and VG-pVE6007-Rev (TAGAACTAGTGGATCCGGCATCAATC CTTGCAGGCAT). The VG-pVE6007-Fwd and VG-pVE6007-Rev primers contain, respectively, a 5′ attachment of 15 bp homologous to the 3′ end of the linearized pVE6007 and a 5′ attachment of 15 bp homologous to the 5′ end of linearized pVE6007. A circular plasmid was obtained by homologous recombination using 100 ng of the *vanG* PCR product and 100 ng of linearized pVE6007 and 10 μl of an In-Fusion HD cloning reaction mixture as instructed by the manufacturer (Clontech PT5162-1). To propagate the constructed plasmid, chemically competent *Escherichia coli* Top-10 cells were subsequently transformed with 3 μl of the reaction mixture and plated on LB agar containing 10 μg/ml of chloramphenicol at 30°C. Transformants with the desired construct were screened by PCR and by electrophoresis analysis of extracted plasmids. GBS-NY competent cells were transformed by electroporation (a single pulse of 2.5 kV, capacitance at 25 μF, and resistance at 200 Ω) with the constructed plasmid purified from *E. coli*. The electroporated cells were plated on prewarmed Todd-Hewitt agar supplemented with 0.5% yeast extract (THYB) and containing 10 μg/ml of chloramphenicol after 2.5 h of incubation in 300 μl of THYB-glycine without drug at 30°C. Transformants were identified at the permissive temperature for plasmid replication (30°C). Single-crossover Campbell-type chromosomal insertions were selected by shifting to the nonpermissive temperature (37°C) while maintaining chloramphenicol selection. The insertion mutants were confirmed by PCR employing appropriate primers annealing to *vanG* and plasmid sequences.

Filter mating. Filter mating experiments were performed as described previously (29). Strains GBS-NY, GBS-NM, and Sa were used as attempted donors. Vancomycin-susceptible, erythromycin-resistant strains of *S. agalactiae* serotypes I, Ia, II (including ST22 control strain GBS6), III, IV, V, VI, VII, VIII, and IX and *E. faecalis* 2003005056 (SS 1297) were used as recipients for GBS-NM and Sa; vancomycin-susceptible and erythromycin-susceptible *E. faecalis* ATCC 19433 and *E. faecalis* 2004015741 (SS 1928) were used as recipients for all three strains. Selection for transconjugants of GBS-NY, GBS-NM, and Sa was attempted on Todd-Hewitt agar containing 0.2% yeast extract, 5% sheep blood/Trypticase soy agar, and M enterococcus medium containing 2 μg/ml vancomycin and/or 5 μg/ml erythromycin (Sigma-Aldrich, St. Louis, MO).

Nucleotide sequence accession numbers. The GenBank accession numbers for the four genomes sequenced in this work are CP007570 (GBS-NY; 2,243,708 bp), CP007571 (GBS-NM; 2,214,307 bp), CP007572 (GBS6; 2,231,475 bp), and CP007573 (Sa; 2,036,353 bp).

SUPPLEMENTAL MATERIAL

Supplemental material for this article may be found at http://mbio.asm.org/lookup/suppl/doi:10.1128/mBio.01386-14/-/DCSupplemental.

Figure S1, PPTX file, 0.1 MB.
Figure S2, PPTX file, 0.1 MB.
Table S1, DOCX file, 0.1 MB.

ACKNOWLEDGMENTS

This research was supported in part by an appointment (B.J.M.) to the Bioinformatics in Public Health (BPH) Fellowship Program administered by the Association of Public Health Laboratories (APHL) and funded by Cooperative Agreement U60HM000803 from the Centers for Disease Control and Prevention (CDC).

We thank Kristen Shaw from the Minnesota Dept. of Public Health for initial identification of the resistant *Streptococcus anginosus* isolate and Ruth Lynfield for supplying clinical information pertaining to this isolate. We also thank all of the Active Bacterial Core surveillance participants for providing the thousands of invasive GBS isolates that have been tested over the past 18 years.

REFERENCES

1. **Krcmery V, Jr, Spanik S, Trupl J.** 1996. First report of vancomycin-resistant *Streptococcus mitis* bacteremia in a leukemic patient after prophylaxis with quinolones and during treatment with vancomycin. J. Chemother. **8:**325–326. http://dx.doi.org/10.1179/joc.1996.8.4.325.
2. **Poyart C, Pierre C, Quesne G, Pron B, Berche P, Trieu-Cuot P.** 1997. Emergence of vancomycin resistance in the genus *Streptococcus*: characterization of a *vanB* transferable determinant in *Streptococcus bovis*. Antimicrob. Agents Chemother. **41:**24–29.
3. **Park C, Nichols M, Schrag SJ.** 2014. Two cases of invasive vancomycin-resistant group B *Streptococcus* infection. N. Engl. J. Med. **370:**885–886. http://dx.doi.org/10.1056/NEJMc1308504.
4. **McKessar SJ, Berry AM, Bell JM, Turnidge JD, Paton JC.** 2000. Genetic characterization of *vanG*, a novel vancomycin resistance locus of *Enterococcus faecalis*. Antimicrob. Agents Chemother. **44:**3224–3228. http://dx.doi.org/10.1128/AAC.44.11.3224-3228.2000.
5. **Depardieu F, Bonora MG, Reynolds PE, Courvalin P.** 2003. The *vanG* glycopeptide resistance operon from *Enterococcus faecalis* revisited. Mol. Microbiol. **50:**931–948. http://dx.doi.org/10.1046/j.1365-2958.2003.03737.x.
6. **Depardieu F, Perichon B, Courvalin P.** 2004. Detection of the van alphabet and identification of enterococci and staphylococci at the species level by multiplex PCR. J. Clin. Microbiol. **42:**5857–5860. http://dx.doi.org/10.1128/JCM.42.12.5857-5860.2004.
7. **Boyd DA, Du T, Hizon R, Kaplen B, Murphy T, Tyler S, Brown S, Jamieson F, Weiss K, Mulvey MR.** 2006. VanG-type vancomycin-resistant Enterococcus faecalis strains isolated in Canada. Antimicrob. Agents Chemother. **50:**2217–2221. http://dx.doi.org/10.1128/AAC.01541-05.
8. **Courvalin P.** 2006. Vancomycin resistance in gram-positive cocci. Clin. Infect. Dis. **42**(Suppl 1):S25–S34. http://dx.doi.org/10.1086/491711.
9. **Domingo MC, Huletsky A, Giroux R, Picard FJ, Bergeron MG.** 2007. *vanD* and *vanG*-like gene clusters in a *Ruminococcus* species isolated from human bowel flora. Antimicrob. Agents Chemother. **51:**4111–4117. http://dx.doi.org/10.1128/AAC.00584-07.
10. **Ammam F, Marvaud JC, Lambert T.** 2012. Distribution of the *vanG*-like gene cluster in *Clostridium difficile* clinical isolates. Can. J. Microbiol. **58:**547–551. http://dx.doi.org/10.1139/w2012-002.
11. **Sieradzki K, Tomasz A.** 1999. Gradual alterations in cell wall structure and metabolism in vancomycin-resistant mutants of *Staphylococcus aureus*. J. Bacteriol. **181:**7566–7570.
12. **Meziane-Cherif D, Saul FA, Haouz A, Courvalin P.** 2012. Structural and functional characterization of VanG D-Ala:D-Ser ligase associated with vancomycin resistance in Enterococcus faecalis. J. Biol. Chem. **287:**37583–37592. http://dx.doi.org/10.1074/jbc.M112.405522.

13. **Brenciani A, Tiberi E, Bacciaglia A, Petrelli D, Varaldo PE, Giovanetti E.** 2011. Two distinct genetic elements are responsible for erm(TR)-mediated erythromycin resistance in tetracycline-susceptible and tetracycline-resistant strains of *Streptococcus pyogenes*. Antimicrob. Agents Chemother. **55:**2106–2112. http://dx.doi.org/10.1128/AAC.01378-10.
14. **Spellerberg B, Pohl B, Haase G, Martin S, Weber-Heynemann J, Lütticken R.** 1999. Identification of genetic determinants for the hemolytic activity of *Streptococcus agalactiae* by ISS1 transposition. J. Bacteriol. **181:**3212–3219.
15. **Pritzlaff CA, Chang JC, Kuo SP, Tamura GS, Rubens CE, Nizet V.** 2001. Genetic basis for the beta-haemolytic/cytolytic activity of group B *Streptococcus*. Mol. Microbiol. **39:**236–247. http://dx.doi.org/10.1046/j.1365-2958.2001.02211.x.
16. **Verani JR, McGee L, Schrag SJ.** 2010. Prevention of perinatal group B streptococcal disease—revised guidelines from CDC, 2010. MMWR Recomm Rep. **59**(RR-10):1–36.
17. **Tettelin H, Masignani V, Cieslewicz MJ, Donati C, Medini D, Ward NL, Angiuoli SV, Crabtree J, Jones AL, Durkin AS, Deboy RT, Davidsen TM, Mora M, Scarselli M, Margarit y Ros I, Peterson JD, Hauser CR, Sundaram JP, Nelson WC, Madupu R, Brinkac LM, Dodson RJ, Rosovitz MJ, Sullivan SA, Daugherty SC, Haft DH, Selengut J, Gwinn ML, Zhou L, Zafar N, Khouri H, Radune D, Dimitrov G, Watkins K, O'Connor KJ, Smith S, Utterback TR, White O, Rubens CE, Grandi G, Madoff LC, Kasper DL, Telford JL, Wessels MR, Rappuoli R, Fraser CM.** 2005. Genome analysis of multiple pathogenic isolates of *Streptococcus agalactiae*: implications for the microbial "pan-genome". Proc. Natl. Acad. Sci. U. S. A. **102:**13950–13955. http://dx.doi.org/10.1073/pnas.0506758102.
18. **Palmieri C, Princivalli MS, Brenciani A, Varaldo PE, Facinelli B.** 2011. Different genetic elements carrying the *tet*(W) gene in two human clinical isolates of *Streptococcus suis*. Antimicrob. Agents Chemother. **55:**631–636. http://dx.doi.org/10.1128/AAC.00965-10.
19. **Shewmaker PL, Steigerwalt AG, Whitney AM, Morey RE, Graziano JC, Facklam RR, Musser KA, Merquior VL, Teixeira LM.** 2012. Evaluation of methods for identification and determination of the taxonomic status of strains belonging to the *Streptococcus porcinus-Streptococcus pseudoporcinus* complex isolated from animal, human, and dairy sources. J. Clin. Microbiol. **50:**3591–3597. http://dx.doi.org/10.1128/JCM.01481-12.
20. **Clinical and Laboratory Standards Institute (CLSI).** 2012. Performance standards for antimicrobial susceptibility testing, p M100–MS21. Clinical and Laboratory Standards Institute, Wayne, PA.
21. **Jeng A, Sakota V, Li Z, Datta V, Beall B, Nizet V.** 2003. Molecular genetic analysis of a group A *Streptococcus* operon encoding serum opacity factor and a novel fibronectin-binding protein, SfbX. J. Bacteriol. **185:**1208–1217. http://dx.doi.org/10.1128/JB.185.4.1208-1217.2003.
22. **Hyatt D, Chen G-L, LoCascio PF, Land ML, Larimer FW, Hauser LJ.** 2010. Prodigal: prokaryotic gene recognition and translation initiation site identification. BMC Bioinformatics **11:**119. http://dx.doi.org/10.1186/1471-2105-11-119.
23. **Fouts DE, Brinkac L, Beck E, Inman J, Sutton G.** 2012. Panoct: automated clustering of orthologs using conserved gene neighborhood for pan-genomic analysis of bacterial strains and closely related species. Nucleic Acids Res. **40:**e172. http://dx.doi.org/10.1093/nar/gks757.
24. **Altschul SF, Gish W, Miller W, Myers EW, Lipman DJ.** 1990. Basic local alignment search tool. J. Mol. Biol. **215:**403–410. http://dx.doi.org/10.1016/S0022-2836(05)80360-2.
25. **Bradley RK, Roberts A, Smoot M, Juvekar S, Do J, Dewey C, Holmes I, Pachter L.** 2009. Fast statistical alignment. PLOS Comput. Biol. **5:**e1000392. http://dx.doi.org/10.1371/journal.pcbi.1000392.
26. **Capella-Gutiérrez S, Silla-Martínez JM, Gabaldón T.** 2009. Trimal: a tool for automated alignment trimming in large-scale phylogenetic analyses. Bioinformatics **25:**1972–1973. http://dx.doi.org/10.1093/bioinformatics/btp348.
27. **Stamatakis A.** 2014. RAxML version 8: a tool for phylogenetic analysis and post-analysis of large phylogenies. Bioinformatics **30:**1312–1313. http://dx.doi.org/10.1093/bioinformatics/btu033.
28. **Maguin E, Duwat P, Hege T, Ehrlich D, Gruss A.** 1992. New thermosensitive plasmid for gram-positive bacteria. J. Bacteriol. **174:**5633–5638.
29. **Poyart-Salmeron C, Carlier C, Trieu-Cuot P, Courtieu AL, Courvalin P.** 1990. Transferable plasmid-mediated antibiotic resistance in *Listeria monocytogenes*. Lancet **335:**1422–1426. http://dx.doi.org/10.1016/0140-6736(90)91447-I.